Electronic Supporting Information

Metal Ion Mediated Electron Transfer at Dye-Semiconductor Interfaces

Jamie C. Wang[§,†], *Kyle Violette*[§,†], *Omotola O. Ogunsolu*[‡], *Kenneth Hanson*[*,†,‡]

[†]Department of Chemistry and Biochemistry, Florida State University, Tallahassee, Florida 32304, United States.

[‡]Materials Science and Engineering, Florida State University, Tallahassee, Florida 32306, United States.

Contents

1. Experimental Details .....Page S-2
2. **Figure S1.** ATR-FTIR absorption spectra .....Page S-8
3. **Figure S2.** Concentration and time dependent RuP loading.....Page S-8
4. **Table S1.** Surface coverage and adsorption constant .....Page S-8
5. **Figure S3.** UV-Vis absorption spectra.....Page S-9
6. **Figure S4.** DPV traces .....Page S-9
7. **Figure S5.** Nanosecond TA spectra .....Page S-10
8. **Figure S6.** Equivalent circuit used to fit the EIS data .....Page S-10
9. **Table S2.** Photophysical and electrochemical properties .....Page S-11
10. **Table S3.** EIS fitting parameters.....Page S-11
11. **References** .....Page S-12

EXPERIMENTAL SECTION

Materials: Fluorine-doped tin oxide (FTO) glass substrates were purchased from Hartford Glass Co. (sheet resistance 15Ω $^{-1}$). Zirconyl chloride octahydrate ($ZrOCl_2.8H_2O$, Sigma Aldrich) and Copper(II) acetate monohydrate ($Cu(OOCCH_3)_2 \cdot H_2O$, Sigma Aldrich) were used as purchased without further purification. Acetonitrile (Aldrich), Dichloromethane (DCM, Aldrich), Methanol (MeOH, Aldrich), Perchloric acid ($HClO_4$, Aldrich) and Ethanol (EtOH, Koptec) solvents were all used without further purification.

Synthesis: **B** (tert-phenyl bisphosphonic acid)[1] and **RuP**[2] were synthesized following literature procedure.

TiO_2 sol-gel preparation: The TiO_2 nanoparticle paste was synthesized by slight modification of literature procedure.[3] 7.3 mL (11 wt%) of Tetraisopropyl Orthotitanate was added dropwise (110 mL/hr) to an ice cooled, rapidly stirring (300 rpm) 125 mL Erlenmeyer flask containing a solution of 0.42 mL nitric acid in 60 mL deionized water. The slurry was stirred for 15 min after which the flask was covered with aluminium foil and heated up to 95^{o}C. The sample was held at this temperature until the volume was reduced, through evaporation, to 18 mL. The solution was placed in an acid digestion vessel (VWR, 25227-094) and heated in a box furnace (Thermo Scientific, BF51866A-1) at 200^{o}C for 10.5 h. Upon cooling to room temperature, the solution was transferred to a glass vial. To the solution, 1g (5.3 wt%) of carbowax copolymer (ground to powder with a mortar and pestle) and the mixture was stirred for another 48 h.

ZrO_2 sol-gel preparation: Zirconium oxide nanoparticle paste was synthesized through similar procedure at TiO_2 with minor differences. 7.2 mL (10.4 wt%) of Zirconium (IV) propoxide (70% in n-propanol) was added dropwise (30 mL/hr) to a stirring (300 rpm) solution of 0.302mL nitric acid in 43.2 mL deionized water. The slurry was continuously stirred for 15 min after which the flask was covered with aluminium flask and heated to 95^{o}C until it was reduced to a volume of 18 mL. As described above, the solution was

heated in a vessel/box oven at 200°C for 10.5 h after which 1.02 g (5.4 wt%) of ground carbowax copolymer was added to the solution and stirred for 48 h.[4]

Film Preparation: FTO glass substrates were sonicated in ethanol and then HCl/Ethanol (15/85% mix) for 20 min. Nanocrystalline TiO_2 films ~2.4 μm thick, coating an area of 5 × 5 mm on top of $TiCl_4$ treated FTO glass were prepared by doctor blading (1 layer of scotch tape) with the TiO_2 paste and subsequently sintered at 500°C for 30 min. The TiO_2-B film was prepared by soaking TiO_2 in a 0.30 mM B in DMSO for 24 hours followed by rinsing with MeOH and drying with a stream of air. Bilayer formation was achieved by stepwise soaking of the thin films. The slides were removed, rinsed with MeOH and dried under a stream of air. Zirconium treatments were performed by immersing the TiO_2-B films in 0.5 mM solution of $ZrOCl_2$ in 0.1M $HClO_4$ for 24 h, followed by subsequent rinsing with MeOH and air drying. Copper treatments were performed by immersing the TiO_2-B films in 0.5 mM solution of $Cu(OOCCH_3)_2 \cdot H_2O$ in DI H_2O for 24 h, followed by subsequent rinsing with MeOH and air drying. Finally, the TiO_2-B-**Zr** and TiO_2-B-**Cu** films were soaked in a solution of RuP dye (0.1 mM) in MeOH for 24 h and rinsed with MeOH to remove unbound RuP dye. The same loading procedure was followed for the ZrO_2 thin films.

Surface Coverage Determination: The surface coverage for the dyes were calculated using the expression $\Gamma = (A(\lambda)/\varepsilon(\lambda))/1000$, where Γ is the surface coverage in mol cm^{-2}, $A(\lambda)$ is the absorbance of the film, and $\varepsilon(\lambda)$ is the aqueous solution extinction coefficient for the dyes, which is 1.26×10^4 $M^{-1}cm^{-1}$ at 456 nm for RuP. Adsorption isotherms (Figure S2) were fit using $\Gamma = K_{ad}((\Gamma_{max} \times [RuP]/(1 + \Gamma_{max} \times [RuP])$ to give the equilibrium adsorption constant (K_{ad}) and maximum surface coverages (Γ_{max}) in accord with the the Langmuir isotherm model.[5]

DSSC Fabrication: The mono- and bi-layer functionalized TiO_2 films on FTO glass (1.4 × 1.9 cm) served as the photo anode of the DSSCs. The cathode was prepared by first drilling a small hole (d = 1.1 mm) into the corner of the 1.9 × 2.1 cm glass slide. The drilled slides were then sonicated with ethanol for 10

minutes. This was followed by deposition of Platinum by drop casting 75 μL of a ~ 4 mM solution of H_2PtCl_6 in ethanol on FTO glass followed by heat treatment (400 °C) using a Leister Hot air Blower. DSSC sandwich cells were prepared using a home-built assembly apparatus.[6] A 2 mm wide 1.2 × 1.2 cm Surlyn thermo plastic (25 μm thick Meltonix 1170−25 from Solaronix) was placed between the anode and the cathode and the entire ensemble heated to ~150 °C for 7 s. The electrolyte (0.6 M BMII, 0.1 M LiI, 0.05 M I_2, 0.1 M GSCN, 0.5 M TBP in a 85:15 mixture of acetonitrile and valeronitrile) was introduced into the cell through a hole on the counter electrode using vacuum backfilling. The cell was then sealed by heating a meltonix film and microcover glass slide (18 × 18 mm VWR).

Film and Device Characterization

Absorption Spectroscopy: The UV−visible spectra were recorded using an Agilent 8453 UV−visible photodiode array spectrophotometer by placing the dry derivatized TiO_2/FTO slides perpendicular to the detection beam path.

Attenuated Total Reflectance Infrared Spectra were recorded using a Bruker Alpha FTIR spectrometer (SiC Glowbar source, DTGS detector) with a Platinum ATR quickSnap sampling module (single reflection diamond crystal). Spectra were acquired from 800 to 1700 cm^{-1} at a resolution of 4 cm^{-1}. All ATR-IR spectra are reported in absorbance with a blank versus atmosphere.

Transient Absorption Measurements: Transient absorption (TA) measurements were carried out by inserting samples (1 × 4 cm glass slides with a 1.5 × 1 cm TiO_2 active area) at a 45° angle into a 10 mm path length square cuvette containing 0.1 M $LiClO_4$ in MeCN. The spectrometer is composed of a Continuum Surelite EX Nd:YAG laser combined with a Continuum Horizon OPO (532 nm, 5-7 ns, operated at 1 Hz, beam diameter ~0.5 cm, 2.5 to 5 mJ/pulse) integrated into a commercially available Edinburgh LP980 laser flash photolysis spectrometer system. White light probe pulses generated by a pulsed 150 W Xe lamp were passed through the sample, focused into the spectrometer (5.5 nm

bandwidth), then detected by intensified Andor iStar CCD camera. Detector outputs were processed using Edinburgh's L900 (version 8.2.3, build 0) software package.

Single wavelength kinetic absorption is detected by a photomultiplier tube with a 532 nm notch filter placed before the detector to reject unwanted scattered light. Detector outputs were processed using a Tektronix TDS3012C Digital Phosphor Oscilloscope interfaced to a PC running Edinburgh's L900 software package. Single wavelength kinetic data were the result of averaging 500 laser shots.

Steady-State and Time-Resolved Emission data were collected at room temperature using an Edinburgh FLS980 spectrometer. Samples were excited using light output from a housed 450 W Xe lamp passed through a single grating (1800 l/mm, 250 nm blaze) Czerny-Turner monochromator, generating 456nm light, and finally a 5 nm bandwidth slit. Emission from the sample was first passed through a 495 nm long-pass color filter, then a single grating (1800 l/mm, 500 nm blaze) Czerny-Turner monochromator (5 nm bandwidth) and finally detected by a peltier-cooled Hamamatsu R928 photomultiplier tube.

The dynamics of emission decay were monitored by using the FLS980's time-correlated single-photon counting capability (1024 channels; 10μs window) with data collection for 10,000 counts. Excitation was provided by an Edinburgh EPL-445 picosecond pulsed diode laser (444.2 nm, 80 ps FWHM) operated at 200 kHz.

Time-resolved emission data were fit by using the bi-exponential function in equation 1. The results of multiple measurements revealed variations in the kinetic fit parameters of 5-10% with general trends reproduced in five separate trials. A weighted average of lifetime τ is calculated by using equation 2.

$$y = A_1 e^{-k1x} + A_2 e^{-k2x} + y_0 \qquad \text{(eq 1)}$$

$$\tau_i = 1/k_i; \langle\tau\rangle = \Sigma A_i \tau_i{}_i^2 / \Sigma A_i \tau \qquad \text{(eq 2)}$$

Emission quantum yields were acquired using an integrating sphere incorporated into a spectrofluorometer (FLS980, Edinburgh Instruments). The samples were prepared in a DSSC sandwich cell-type architecture as depicted in Figure S2 of previous literature.[7] FTO glass was cut into 2 × 2 cm squares and an active area of 1 cm^2 metal oxide was prepared by doctor blading and dye loading as

described above. A small hole (d = 1.1 mm) was drilled into the corner of the 2 × 2 cm glass slide that did not have metal oxide. A 1 mm wide 2 × 2 cm Meltonix film (1170-25 from Solaronix) was placed between the two glass slides and the entire ensamble heated to ~150°C for 7 seconds. After cooling to room temperature, 0.3M $LiOCl_4$ in MeCN was then injected through the 1 mm hole to fill the interior of the slides using a Vac'n Fill Syringe (65209 from Solaronix). The cell was then sealed with a meltonix flim and micro glass cover slide (18×18mm VWR) that covered the hole used for solvent injection. The final sandwich cell was then placed on the solid sample holder as depicted in Figure S3. TiO_2 and ZrO_2 cells without **RuP** were used as the reference for excitation scatter/absorption and emission.

Emission quantum yields were acquired following literature procedure with minor modification.[8] Because the emission intensity from quenched samples was low (<1%) we adopted a procedure described by Askes et al.[9] In this procedure, absorption/scatter at the excitation wavelength and emission from the sample/reference were acquired under the same instrument settings (λ_{ex} = 456 nm; 5 nm excitation slit; 0.3 nm emission slit; scan 451-461 nm for scatter/absorption; scan 500-850 nm for emission). However, the absorption/scatter scans were measured with a neutral density filter, with known absorption (OD = 3; 0.1 % transmittance), placed between the integrating sphere and the monochrometer/detector. The filter was then removed for the emission scans. The integrated area for scatter/absorption was multiplied by 1000 to correct for the filter attenuation. Quantum yields were then calculated by using the Edinburg L980 software package.

Differential Pulse Voltammetry. Differential pulse voltammetry (DPV) measurements were performed by using a CH Instruments Model CHI620E Series Electrochemical Workstation with the TiO_2-**RuP**, TiO_2-B-**Zr-RuP** or TiO_2-B-**Cu-RuP** films as the working electrode, a platinum wire counter electrode and a Ag wire reference electrode. All measurements were performed in 0.1 M $TBAPF_6$ acetonitrile solution with ferrocene as an internal standard. All potentials have been converted and reported with respect to the normal hydrogen electrode (with Fc^+/Fc being 630 mV relative to NHE).

Devices Characterization: The photocurrent-voltage curves (J-V curves), incident photon-to-current efficiencies (IPCE), and electrochemical impedance spectroscopy (EIS) were measured following our previous published procedures.[6]

Photocurrent-Voltage Curves: The Power Conversion Efficiencies (PCE) of the DSSCs were measured by irradiating the devices with an AM1.5 Solar Spectrum generated from a 300 W xenon arc lamp (Ushio, UXL-302-O) enclosed in a Oriel Research Arc lamp Housing (Newport, 67005) with the light output passed through an AM 1.5 Global filter (Newport, 81094) and mechanical shutter (Newport, 71445). Current−voltage (I−V) relationship was measured using a Keithley Model 2400 Source Meter. The light intensity was measured using a calibrated reference cell and meter (Newport, 91150 V). [6]

Incident Photon to Current Efficiency: IPCE measurements were performed using light from the 300 W xenon lamp passed through a Cornerstone 260 monochromator (Newport, 74125) onto the cells and the light scanned from 300 to 800 nm in 5 nm intervals. Incident light intensity and photocurrent were measured using power meter (Newport, 2936-C) and Oriel 71580 Silicon Detector Head (Newport). [6]

Electrochemical Impedance Spectroscopy: EIS (Gamry Instruments, Interface 1000) was performed scanning from 10^6 Hz to 0.025 Hz with a perturbation amplitude of 10 mV after conditioning the cells for 15 s and allowing an initial delay of 50 s. Measurements were performed at open circuit voltage. The Nyquist and Bode plots were fit by using the Gamry Echem Analyst Software using the equivalent circuit shown in Figure S6 in accord with a previously published procedure.[6, 10]

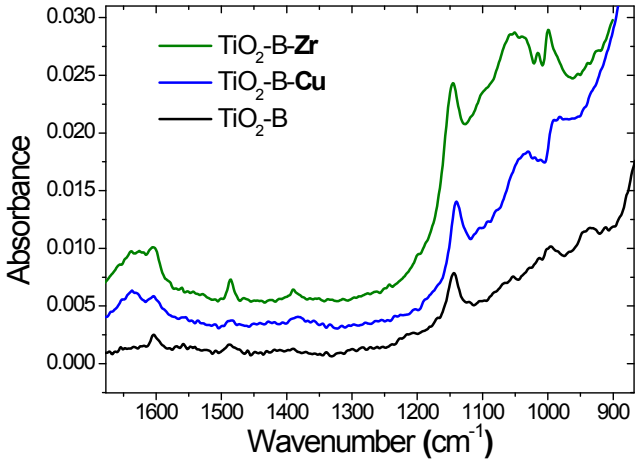

Figure S1. ATR-FTIR absorption spectra for TiO_2-B before and after loading with Zr^{4+} and Cu^{2+} ions.

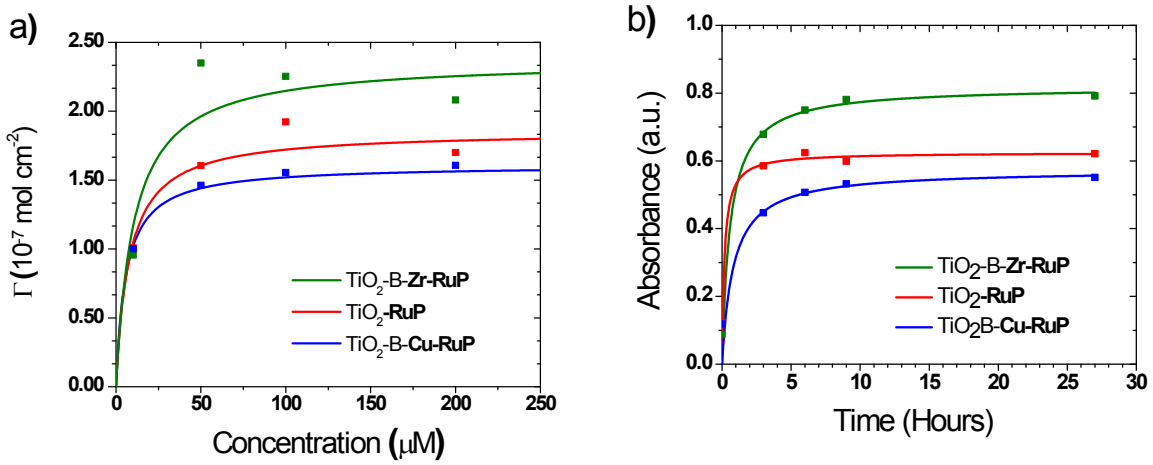

Figure S2. UV-Vis absorption intensity at 456 nm for TiO_2, TiO_2-B-**Cu**, and TiO_2-B-**Zr** films loaded from a) various concentrations of RuP in MeOH and b) 100 μm of RuP in MeOH monitored over 27 hours. Data was fit to the Lagmuir isotherm model (solid lines).

Table S1. Maximum surface coverage of RuP and the adsorption equilibrium for each film (3.5 μm thick).

Film	Γ_{max} (× 10^{-8}mol·cm^{-2})[a]	K_{ad} (μ mol·s^{-1})[b]
TiO_2-**RuP**	1.86	0.13
TiO_2-B-**Cu-RuP**	1.61	0.17
TiO_2-B-**Zr-RuP**	2.37	0.10

[a]Γ_{max} = maximum surface coverage and [b]K_{ad} = equilibrium adsorption constant. Values are calculated by fitting the data from **Figure S2a** with the following equation: $y = \Gamma_{max}\frac{K_{ad}\cdot x}{1 + (K_{ad}\cdot x)}$

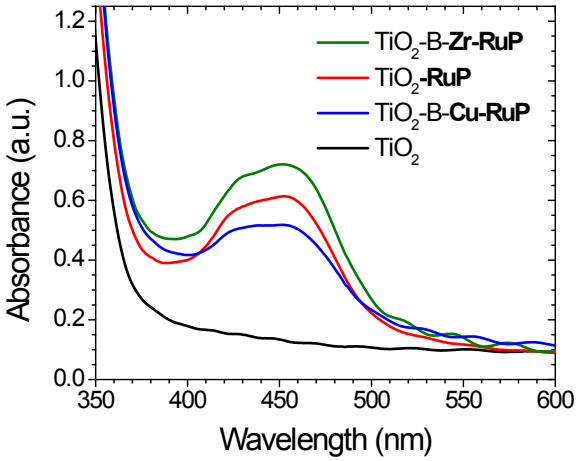

Figure S3. UV-Vis absorption spectra of TiO_2, TiO_2-**RuP**, and TiO_2-B-**M-RuP**.

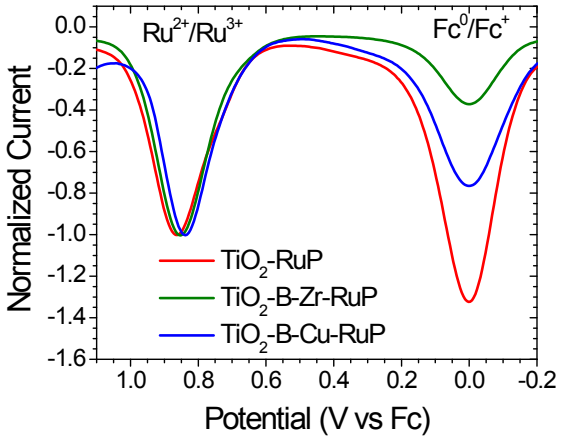

Figure S4. DPV traces of TiO_2-**RuP** and TiO_2-B-**M-RuP** in a 0.1M TBA PF_6 MeCN solution with ferrocene as the internal reference.

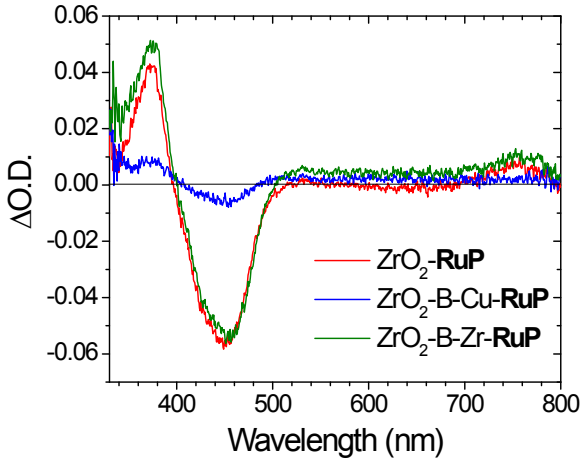

Figure S5. Nanosecond transient absorption spectra of ZrO_2-**RuP** and ZrO_2-B-**M**-**RuP** in MeCN solution 10 ns after laser excitation. (λ_{ex} = 532 nm)

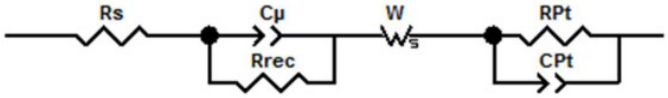

Figure S6. Equivalent circuit used to fit the electrochemical impedance data.

Table S2. Photophysical properties of ZrO_2-**RuP**, TiO_2-**RuP**, ZrO_2-B-**M-RuP,** and TiO_2-B-**M-RuP** in a MeCN solution of 0.3 M $LiClO_4$.

Film	Φ_{PL} (%)[a]	<τ> (ns)[b]	λ_{em} (nm)[c]	$E_{1/2}(Ru^{III/II})$[d,e]	E^{0-0} (eV)[f]	E^o ($Ru^{III/II*}$)[g]
ZrO_2-**RuP**	4.6	516	650	1.50 V	2.14	-0.64 V
ZrO_2-B-**Cu-RuP**	-	52	650	1.45	2.14	-0.69
ZrO_2-B-**Zr-RuP**	4.6	516	650	1.50	2.14	-0.64
TiO_2-B-**Cu-RuP**	-	52	650	1.47	2.14	-0.67
TiO_2-B-**Zr-RuP**	0.7	410	650	1.49	2.14	-0.65
TiO_2-**RuP**	-	230	650	1.50	2.14	-0.64

[a]Measured using an integrating sphere, [b]weighted average lifetime from the biexponential fit (λ_{ex} = 445 nm), [c]for non-emitting samples TiO_2-**RuP**, TiO_2-B-**Cu-RuP** and ZrO_2-B-**Cu-RuP** the emission energy is assumed to be the same as ZrO_2-**RuP** and ZrO_2-B-Zr-RuP, [d] measured using differential pulse voltammetry with an FTO/TiO_2 mono-/bilayer working electrode, a Pt-wire counter electrode, and a silver wire reference electrode with ferrocene as the internal reference. [e]The measured values are reported vs NHE by using Fc/Fc^+ = 0.64V vs. NHE, [f]Determined from the x intercept for the tangent to the inflection point on the high energy side of the emission peak for ZrO_2-RuP, and [g]E^o ($Ru^{III/II*}$) = $E_{1/2}(Ru^{III/II})$ - E^{0-0}.

Table S3. Parameters obtained from fitting the Nyquist Plots with the equivalent circuit shown in Figure S6.

Film	R_{Pt} (Ω)[a]	C_{Pt} (× 10^{-5}F)[a]	R_k (Ω)[a]	C_μ (× 10^{-4} F)[a]	$k_{eff} = \omega_k (s^{-1})$[b]	τ_{eff} (ms)[c]
TiO_2-**RuP**	0.6	32	85.4	1.3	90.4	11.1
TiO_2-B-**Cu-RuP**	1.6	0.8	513.8	0.2	199.0	5.0
TiO_2-B-**Zr-RuP**	3.2	4.2	111.6	2.4	49.5	20.2

R_{Pt} and R_k are the diameters of the high and intermediate frequency arcs respectively in Figure 5b but were also obtained from the equivalent circuit modelling process with Gamry Software along with C_{Pt} and C_μ [b]$k_{eff} = 2\pi f$, and [c]$k_{eff} = 1/\tau_{eff}$.

References

1. (a) Henn, M.; Deáky, V.; Krabbe, S.; Schürmann, M.; Prosenc, Marc H.; Herres-Pawlis, S.; Mahieu, B.; Jurkschat, K., *Z. Anorg. Allg. Chem.* **2011,** *637* (2), 211-223; (b) Prochniak, G.; Zon, J.; Daszkiewicz, M.; Pietraszko, A.; Videnova-Adrabinska, V., *Acta Crystallographica Section C* **2007,** *63* (7), o434-o436; (c) Lo, C.-Y.; Chen, C.-H.; Tsai, T. W. T.; Zhang, L.; Lim, T.-S.; Fann, W.; Chan, J. C. C.; Luh, T.-Y., *J. Chin. Chem. Soc.* **2010,** *57* (3B), 539-546.
2. Norris, M. R.; Concepcion, J. J.; Glasson, C. R. K.; Fang, Z.; Lapides, A. M.; Ashford, D. L.; Templeton, J. L.; Meyer, T. J., *Inorg. Chem.* **2013,** *52* (21), 12492-12501.
3. Lee, S. H.; Abrams, N. M.; Hoertz, P. G.; Barber, G. D.; Halaoui, L. I.; Mallouk, T. E., *J. Phys. Chem. B* **2008,** *112* (46), 14415-21.
4. Song, W.; Glasson, C. R. K.; Luo, H.; Hanson, K.; Brennaman, M. K.; Concepcion, J. J.; Meyer, T. J., *J. Phys. Chem. Lett.* **2011,** *2* (14), 1808-1813.
5. Langmuir, I., *J. Am. Chem. Soc.* **1918,** *40*, 1361.
6. Ogunsolu, O. O.; Wang, J. C.; Hanson, K., *ACS Appl. Mater. Interfaces* **2015,** *7* (50), 27730-27734.
7. Wang, J. C.; Murphy, I. A.; Hanson, K., *J. Phys. Chem. C* **2015,** *119* (7), 3502-3508.
8. McNeil, I. J.; Ashford, D. L.; Luo, H.; Fecko, C. J., *J. Phys. Chem. C* **2012,** *116* (30), 15888-15899.
9. Askes, S. H. C.; Bahreman, A.; Bonnet, S., *Angew. Chem. Int. Ed.* **2014,** *53* (4), 1029-1033.
10. (a) Bisquert, J.; Fabregat-Santiago, F., *Dye-Sensitized Solar Cells* **2010**, 457; (b) Fabregat-Santiago, F.; Bisquert, J.; Garcia-Belmonte, G.; Boschloo, G.; Hagfeldt, A., *Sol. Energy Mater. Sol. Cells* **2005,** *87* (1–4), 117-131; (c) Fabregat-Santiago, F.; Garcia-Belmonte, G.; Mora-Sero, I.; Bisquert, J., *Phys. Chem. Chem. Phys.* **2011,** *13* (20), 9083-9118.